



Remote Sensing for Earth Observation and Surveillance

Homework 2

Adrian Burton Parisi

10710691 | 940789

adrianburton.parisi@mail.polimi.it

1 SAR from Scratch

The following SAR platform will be developed with the following requirements, restrictions, and operational values:

- Ground resolution of $3\text{m} \times 3\text{m}$
- Noise Equivalent Sigma Zero $\sigma_{NESZ}^0 = -22\text{dB}$
- Ground range swath $>40\text{km}$
- Receiver noise figure $F_{dB} = 5\text{dB}$
- Antenna efficiency $\eta = 0.7$
- Transmission duty cycle $<20\%$ of Pulse Repetition Interval (PRI)
- Central frequency $\nu_0 = 9.65\text{GHz}$
- Incidence angle $\theta = 30^\circ$
- Orbiting within a Low Earth Orbit

- 1.1 Determine all relevant system parameters, including: approximate antenna size, radiated peak power, transmitted bandwidth, transmitted pulse duration, Pulse Repetition Frequency, and length of synthetic aperture.

The Noise Power Spectral Density, N_0 , was chosen as the starting point for the calculations and was determined as follows. Firstly, the reference temperature, T_{ref} , scene temperature, T_{sc} , and physical temperature of the antenna, T_{ant_0} , were all set as 288K. This choice for T_{ref} and T_{sc} can be seen as trivial however, the value for T_{ant_0} is based upon that satellites still operate at temperature relatively close to room temperate as certain components should not deviate greatly from this and thus, thermal design is carried out to approximately maintain this temperature.

The noise factor, F , was computed using

$$F = 10^{\frac{F_{dB}}{10}} = 3.1623 \quad (1)$$

where F_{dB} is the provided *receiver noise figure*. Thus, the receiver temperature, T_{rx} , antenna temperature, T_{ant} , and system temperature, T_{sys} , are given by

$$T_{rx} = (F - 1) T_{ref} = 622.7\text{K} \quad (2)$$

$$T_{ant} = \eta T_{sc} + (1 - \eta) T_{ant_0} = 288\text{K} \quad (3)$$

$$T_{sys} = T_{ant} + T_{rx} = 910.7\text{K} \quad (4)$$

Compiling these values together it is now possible to calculate N_0 with

$$N_0 = k_B T_{sys} = 1.257 \times 10^{-20} \left[\frac{\text{W}}{\text{Hz}} \right] \quad (5)$$

where k_B is the Boltzmann constant. Finally, for completeness the noise power was found to be $1.25 \times 10^{-12} \text{W}$.

With a wave speed propagation of the speed of light, c , and given carrier frequency ν_0 , the wavelength, λ , is found to be 3.11cm. A required resolution, ρ , of 3m both in the range and azimuthal directions fixes both the bandwidth, B , and antenna length, L_x , with

$$\Delta r = \rho \sin(\theta) \quad (6)$$

$$B = \frac{c}{2\Delta r} = 100 \text{MHz} \quad (7)$$

$$L_x = 2\rho = 6 \text{m} \quad (8)$$

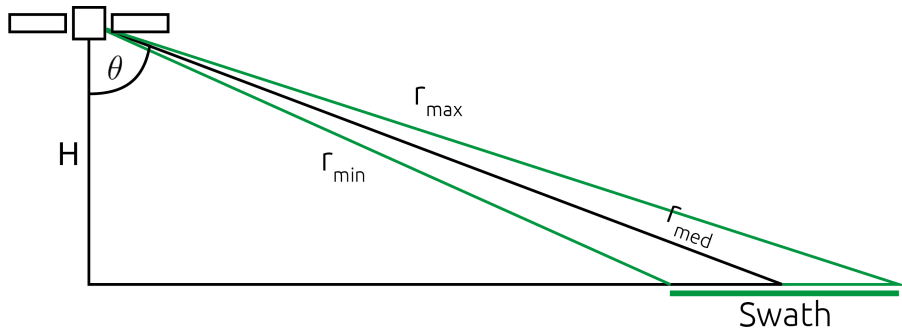


Figure 1: Diagram depicting the different ranges possible for the chosen swath, altitude, and incident angle.

Following this the antenna width, L_z , was determined by using the difference between the angles created by r_{min} and r_{max} resulting in $\Delta\theta$, where the chosen swath is 45km leading to

$$L_z = \frac{\lambda}{\Delta\theta} = 0.369 \text{m} \quad (9)$$

The altitude used, 700km, within this calculation mimics that of the Sentinel-1 satellite, an earth observation platform which is part of the Copernicus program. Proceeding this, the antenna area, A , was found to be 2.21m^2 . This SAR instrument, like the most recent ones, will have a planar antenna. Accordingly, the equation and values for the gain, G , and effective area A_e are determined by

$$G = \eta \frac{4\pi A}{\lambda^2} = 20121 \quad (10)$$

$$A_e = \frac{\lambda^2 G}{4\pi} = 1.548 \text{m}^2 \quad (11)$$

The synthetic aperture, A_s , or maximum synthetic aperture in this case, is calculated via

$$A_s = \frac{\lambda}{L_x r_{max}} = 2.456 \text{km} \quad (12)$$

The PRI depends on the spatial sampling of the synthetic aperture, dx_{ant} which is provided by $dx_{ant} = \rho/2$. Following through, the PRI is given by

$$\text{PRI} = \frac{dx_{ant}}{v} = \frac{\rho}{2v} = 195.5 \mu\text{s} \quad (13)$$

$$\Delta x = \frac{\lambda r_{med}}{2A_s} \quad (14)$$

$$\text{PRI} > \frac{2(r_{max} - r_{min})}{c} \quad (15)$$

$$\text{PRI} < \frac{\Delta x}{v} \quad (16)$$

To ensure that the system is also able to reject range and along track ambiguities Eq. 15 and Eq. 16 were employed, respectively. Both were found to be satisfied. The Pulse Repetition Frequency (PRF) can simply be found by inverting the PRI resulting in a value of 5.12kHz. A duty cycle of 17.5% was chosen leading to a pulse duration, T_g , of 34.2 μ s and the number of effective pulses, N_τ , computed with

$$N_\tau = \frac{A_s}{\text{PRI}v} = 1636 \quad (17)$$

Finally, the peak power transmitted, P_{tx} , can be computed by compiling the majority of previously found values and substituting them into

$$P_{tx} = \frac{\sin(\theta)}{\Delta x \Delta r} \frac{N_0 (4\pi r_{med}^2)^2}{N_\tau T_g \sigma_{NESZ}^0 G A_e} = 936.3 \text{W} \quad (18)$$

with σ_{NESZ}^0 being converted from dB in a similar fashion to that shown in Eq. 1.

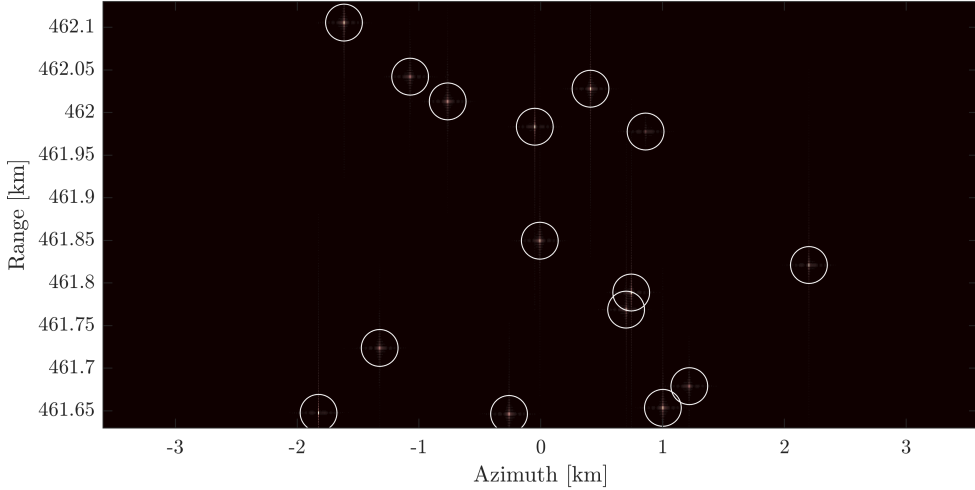


Figure 2: Focused image using a Time Domain Back Projection algorithm with simulated range compressed data.

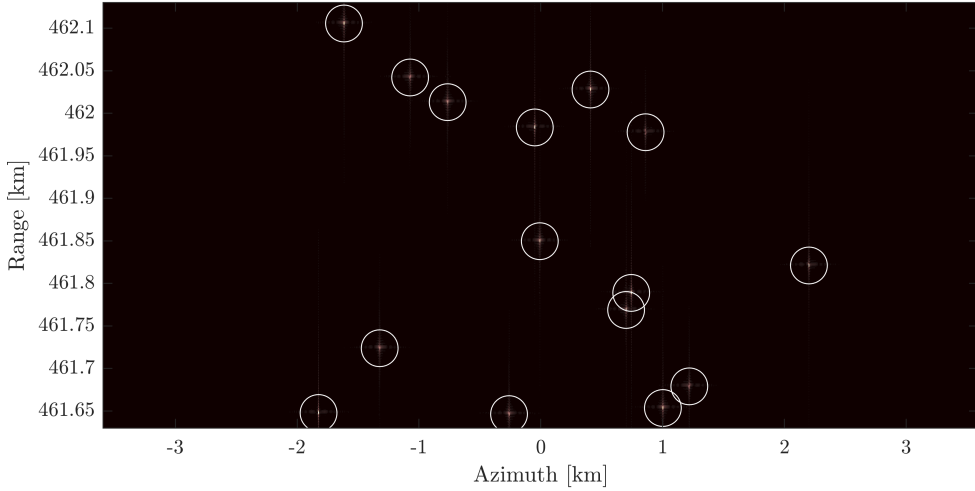


Figure 3: Focused image using an Along Track Cross Correlation algorithm with simulated range compressed data.

In addition, a brief analysis to discover if range migration is present within future acquired data was conducted. This consisted of performing a simulation on a single target, analysing the range compressed data, and comparing against the usual metric for determining if range migration occurs,

$$r < \frac{c}{2B} \quad (19)$$

Simulating only one target simplifies this process as the maximum per row can be taken to show the entire *curve* representing the target and the index for this maximum stored. Each pixel within the simulated image corresponds to a value of 0.75m and calculating the limit for range migration for this case using Eq. 19 results in 1.5m. Therefore, comparing the index for the found maximums can highlight the presence of range migration. With an antenna pattern represented by a cardinal sine, range migration was found. This however, is a simulated result and must be verified during the experimental phase of the instrument design.

1.2 Discuss the choice of the focusing processor.

The choice of the focusing processor will be based solely on the accuracy of the focused data and under the assumption that the processing will occur on ground after data transmission rather than on board computers. This choice opens the possibility of processing this raw data without the limitation of computational power as large computer grids or supercomputers are available to use to exploit parallel based algorithms.[1] As aforementioned the chosen algorithm will be based on accuracy with an aim for achieving the most accurate image possible. As a Time Domain Back Projection (TDBP) algorithm, as stated by Tebaldini et al, is an exact approach even for strongly non-linear cases, this was used as the main comparison if an alternative algorithm should be chosen.[3][4]

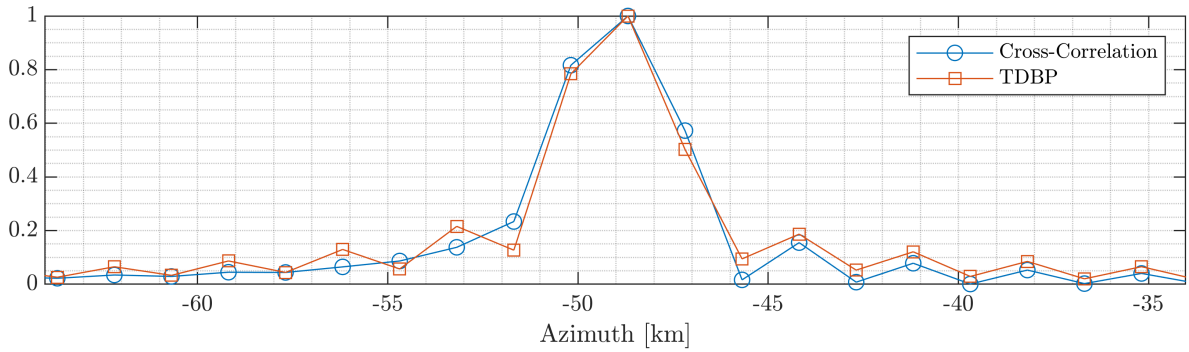


Figure 4: A zoomed in comparison between focusing the simulated data with Along-Track Cross Correlation and Time Domain Back Projection algorithms.

An alternative to Back Projection (BP) algorithms is the Along-Track Cross-Correlation (ATCC) algorithm which can approximate the TDBP algorithm in some cases with a highly reduced computational time. However, in order to compare these a simulation has been performed with a swath of 1km, due to limited computational power, with the same parameters as described in Sect. 1.1, and 15 targets. A focused image for both a TDBP and ATCC has been generated and shown in Figure 2 and 3, respectively. From a simple visual analysis the images can be said to be very similar however, further analysing a column of the same index within both images results in Figure 4. Although the ATCC algorithm produces a decent approximation, if pure accuracy is required then a BP algorithm should be chosen. Therefore, for now the TDBP algorithm will be chosen with future work studying the additional algorithms such as the Filtered Back Projection (FBP) or Fast Factorised Back Projection (FFBP) algorithms with the hopes to ease computational requirements whilst maintaining a high accuracy.[2][4]

- 1.3 Your design is so good that the Space Agency decides to build a second system identical to the first one. The second satellite is assumed to be flown in close formation with the first one, in such a way as to form an interferometric baseline. Discuss how to set the orbital separation between the two satellites to optimise the estimation of terrain topography, and evaluate the expected estimation accuracy assuming a reference backscatter value $\sigma^0 = -15\text{dB}$.

For the purpose of this analysis the assumption that the satellites perform data acquisition at the same time has been put in place. Furthermore, a sole focus has been made to analyse how to minimise the estimation accuracy of the terrain topography, σ_z , neglecting detailed analysis of the other parameters at the current time. The initial step in determining a value of the estimation of the terrain topography is calculating the InSAR coherence, γ , which is built from a product of several decorrelation sources: the system noise γ_{SNR} , the revisit time $\gamma_{temporal}$, the system bandwidth and InSAR baseline $\gamma_{terrain}$, and InSAR baseline γ_{volume} .

$$\gamma = \gamma_{SNR} \gamma_{temporal} \gamma_{terrain} \gamma_{volume} \quad (20)$$

Following the assumption of data acquisition being performed at the same time. As $\gamma_{temporal}$ is defined as

$$\gamma_{temporal} = \exp\left(-\frac{T}{\tau}\right) \quad (21)$$

with revisit period essentially null therefore, this term becomes unity. Furthermore, assuming a bare surface with no vegetation γ_{volume} is also equal to unity. Therefore, this leaves γ_{SNR} and $\gamma_{terrain}$. Both can easily calculated using

$$\gamma_{SNR} = \frac{SNR}{1 + SNR} \quad (22)$$

$$\gamma_{terrain} = \left(1 - \left|\frac{b}{b_{critical}}\right|\right) \quad (23)$$

with

$$b_{critical} = \frac{B}{\nu_0} r_{med} \tan(\theta) = 2.763\text{km}$$

Using the provided information, the Single to Noise Ratio (SNR) was found to be

$$SNR_{dB} = \sigma^0 - \sigma^0_{NESZ} = 7\text{dB} \quad (24)$$

For InSAR, the Cramer Rao Bound (CRB) is generally accepted as a reliable approximation for the phase noise variance, σ_ψ , if the value L_{eq} , the equivalent number of uncorrelated pixels within the averaging window, is taken. Therefore, a value of L_{eq} of 25 was found with a sampling size of $15 \times 15\text{m}$, and the imposed resolution from Sect. 1.1 leading to a value of σ_ψ determined from CRB being,

$$\sigma_\psi = \sqrt{\frac{1 - \gamma^2}{2L_{eq}\gamma^2}} \quad (25)$$

Proceeding this, terrain tomography accuracy, σ_z , is found by first establishing a value for the height-to-phase conversion factor, k_z , then a final calculation for σ_z .

$$k_z = \frac{4\pi}{\lambda} \frac{b}{r \sin(\theta)} \quad (26)$$

$$\sigma_z = \frac{\sigma_\psi}{k_z} \quad (27)$$

Finally, with the tools to calculate a value for σ_z for a given baseline, a minimisation algorithm can be developed. The algorithm is simple and follows the procedure of creating a linear vector of baselines between the values of 0 and $b_{critical}$ and computing the corresponding σ_z for each of these baselines. The minimum σ_z of these calculated values was found to be 0.1259, with σ_ϕ being 0.2669, and the baseline corresponding to these values to be 1.211km.

2 SAR Processing

2.1 Focus the raw data to produce a focused SAR image.

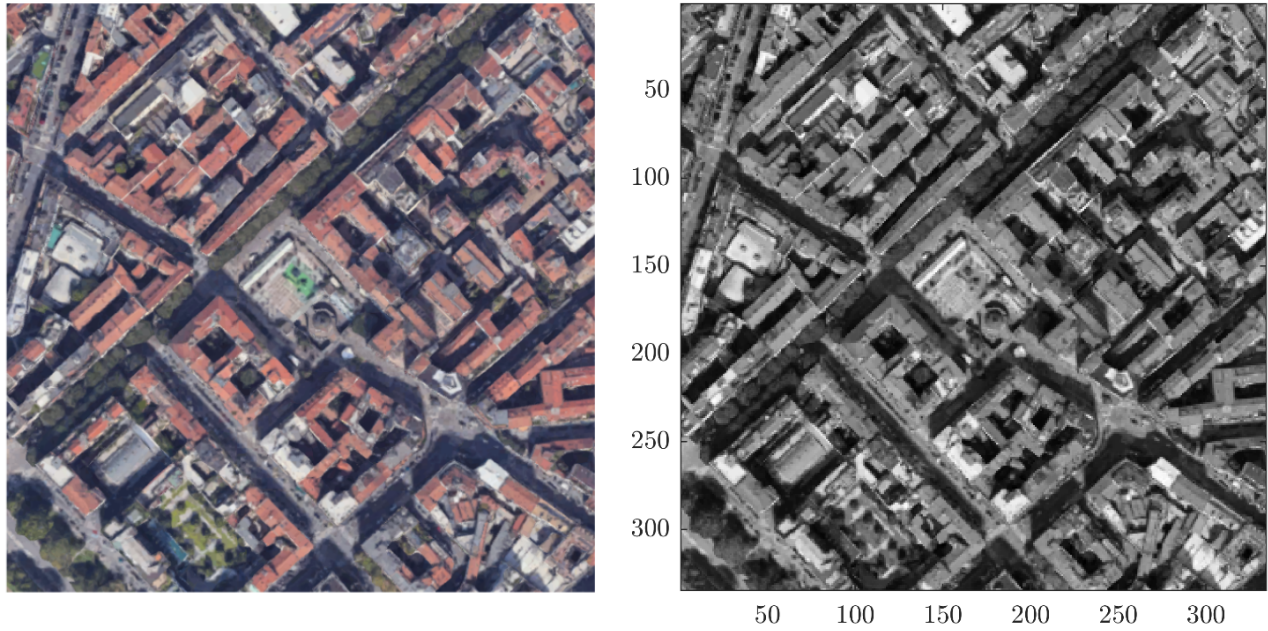


Figure 5: Satellite image of Piazza Antonio Gramsci, Milano. 5 minute walk from Acro della Pace. On the left shows the provided "raw" image to the generator function and the right is the image to project to SAR data.

In order to focus raw data to achieve a focused SAR image, raw data is required. This was achieved by providing an image to the given Matlab function, `Generate_raw_SAR_data`. This function generates dummy SAR data from an image in which SAR processing can be performed. Figure 5 shows the input image on the left with the *target* image processed by `Generate_raw_SAR_data` prior to projecting to dummy SAR data. Furthermore, the function produces a struct with the following data:

- `t_ax` - Fast time [s]
- `xa` - Sensor position along orbit [m]
- `g` - Transmitted pulse
- `r_ax` - Range position to the target [m]
- `f0` - Carrier frequency [Hz]
- `As` - Synthetic Aperture Length [m]
- `B` - Bandwidth [Hz]

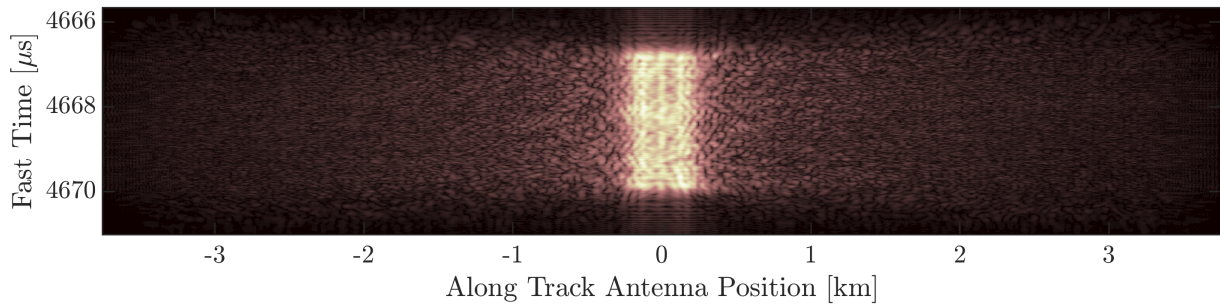


Figure 6: Raw SAR data generated from the image shown in Figure 5

The projected raw SAR data was normalised and can be seen in Figure 6. This SAR data was range compressed by performing a convolution, column by column, with the transmitted pulse or chirp denoted $g(t)$. Prior to range compression a brief analysis was conducted on the transmitted pulse with

the time domain representation shown in Figure 7 and frequency in Figure 8. Additional padding of zeros either side of the chirp have been added in order to cleanly view the pulse. The range compressed signal is shown in Figure 9.

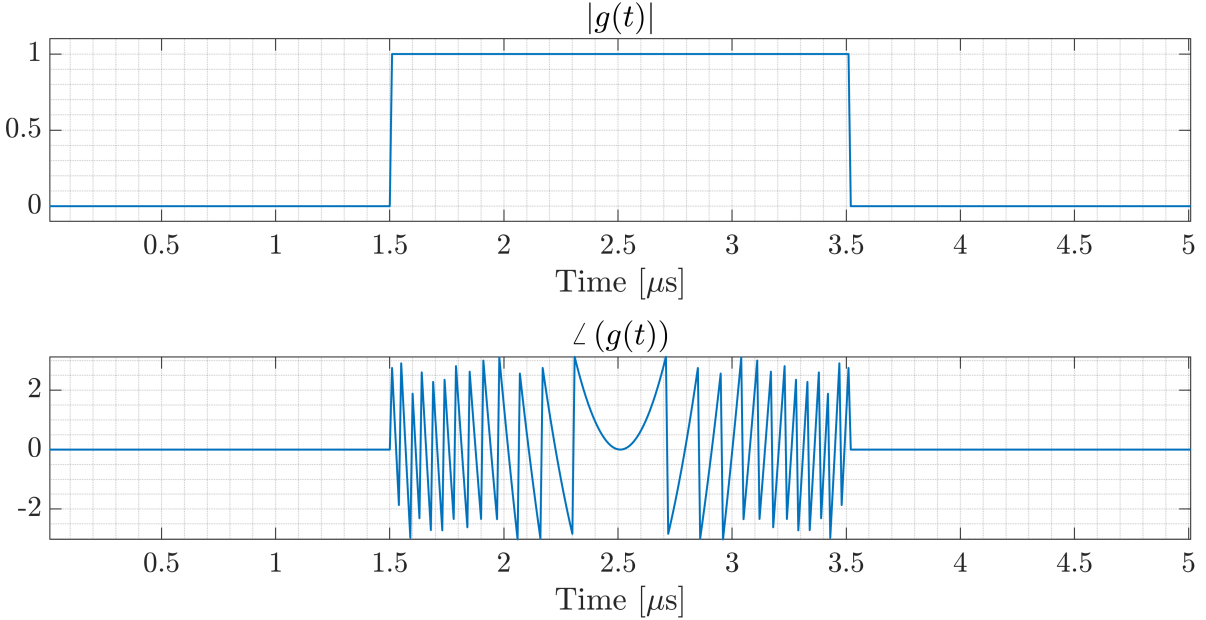


Figure 7: Time domain representation of the transmitted pulse, $g(t)$

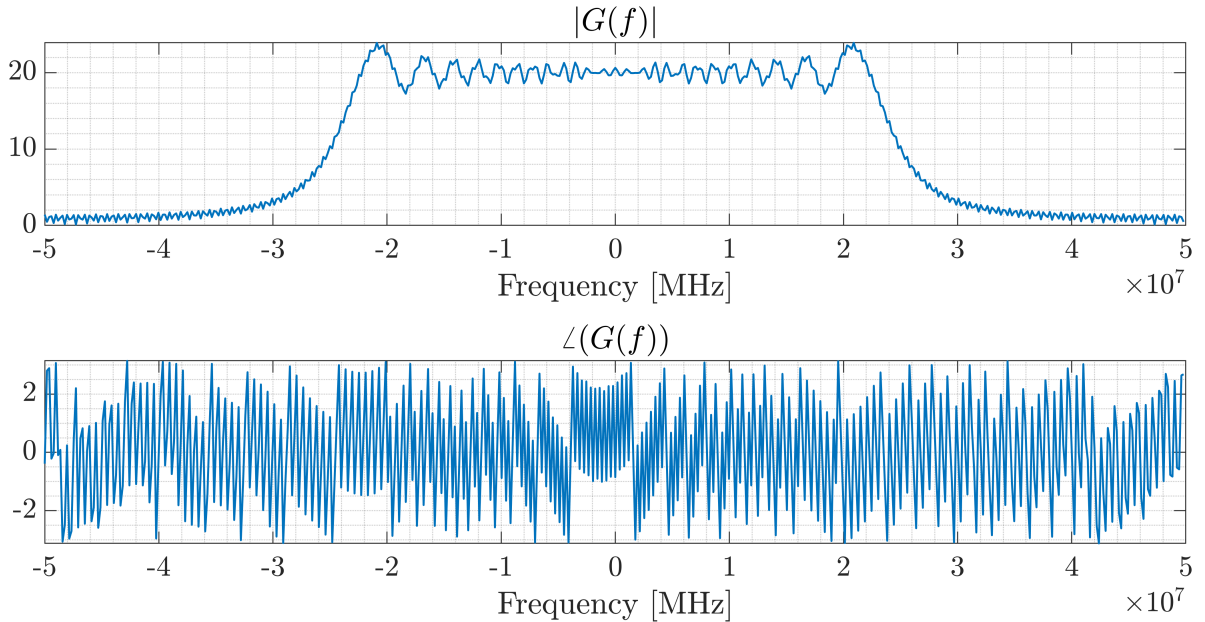


Figure 8: Frequency domain representation of the transmitted pulse generated from a Fourier transform of the signal shown in Figure 7

The range compressed signal was subsequently focused using both the ATCC algorithm with the result shown in Figures 10 and 13a and the TDBP algorithm as shown in Figures 11 and 14a.

2.2 Comment on the choice of the focusing algorithm and its performance in terms of image quality and computational burden.

The following analysis is based on the assumption that the focusing of the range compressed data is being performed on-board the satellite and therefore, is bound by computational and power limits. With this in mind both accuracy and computational time are used as the main parameters to compare

against when choosing a focusing algorithm.

The main choices currently available for the focusing algorithm are the ATCC and the TDBP algorithms. Conducting a brief comparison regarding CPU time showed that the ATCC algorithm required ≈ 1 second to compute with the TDBP demanding a computational time of ≈ 10 minutes.¹

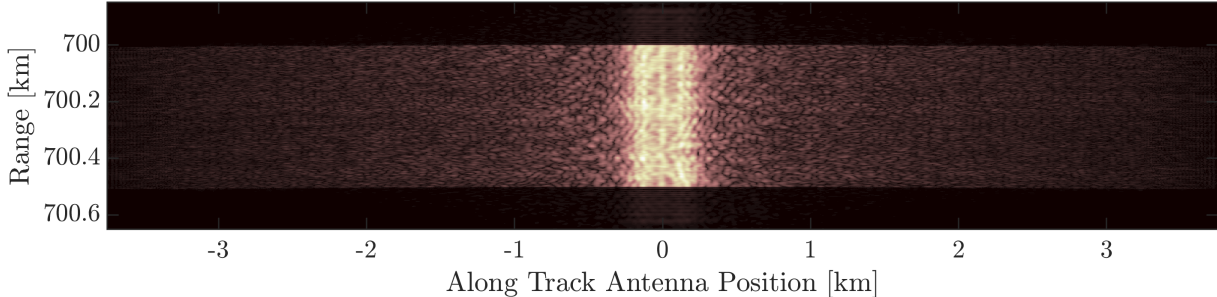


Figure 9: The SAR data post range compression

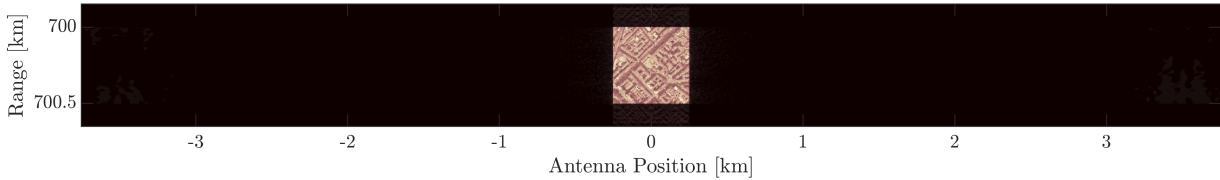


Figure 10: Focused image using the Along Track Cross Correlation algorithm on the range compressed SAR data as shown in Figure 9.

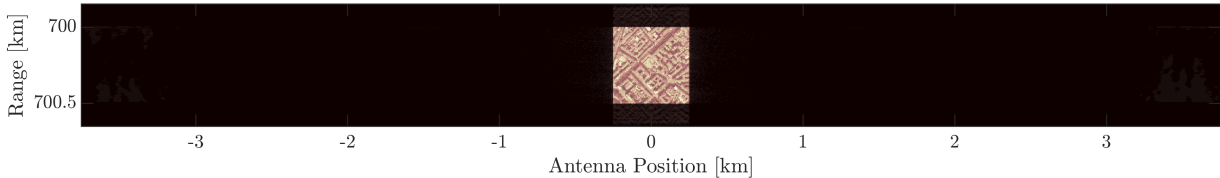


Figure 11: Focused image using the Time Domain Back Projection algorithm on the range compressed SAR data as shown in Figure 9.

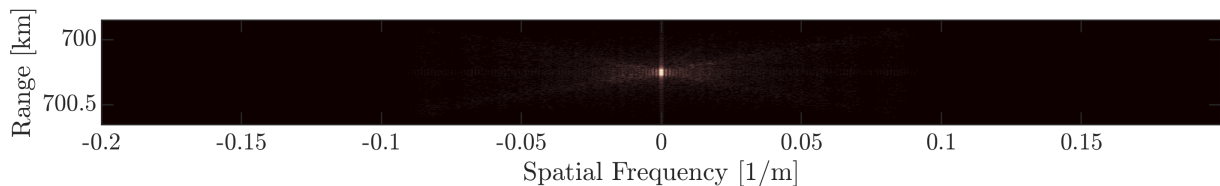


Figure 12: Focused image using the Discrete Fourier Transform algorithm on the range compressed SAR data as shown in Figure 9.

Furthermore, focusing the image by Discrete Fourier Transform (DFT) was briefly considered and performed with the results shown in Figure 12. Comparing the final imagery between Figures 10 and 12 it is clear that the DFT algorithm, although requiring similar computational time compared to the ATCC algorithm, provides non-optimal results with the final image not resembling any form of the

¹Computed on a Surface Book 2 i7-8650U running on battery

initial input image and therefore can't be used. This was the expectation for not having DFT as an initial candidate however, this analysis has confirmed this reasoning.

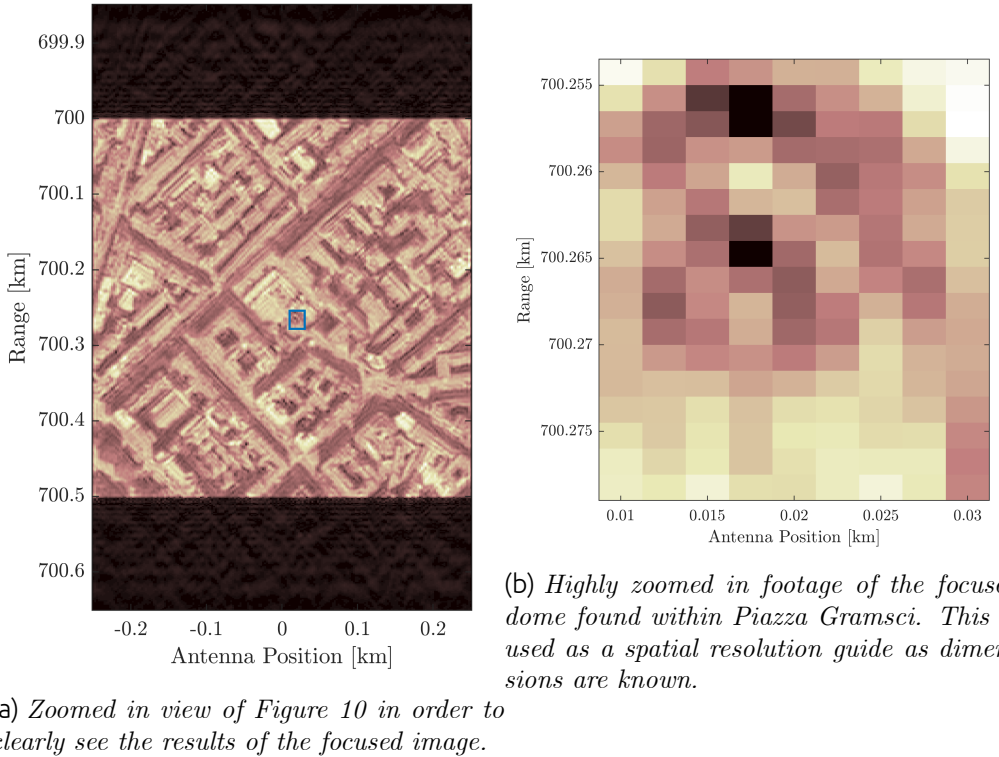


Figure 13: The final focused image for the given input as shown in Figure 5 using the Along Track Cross Correlation algorithm.

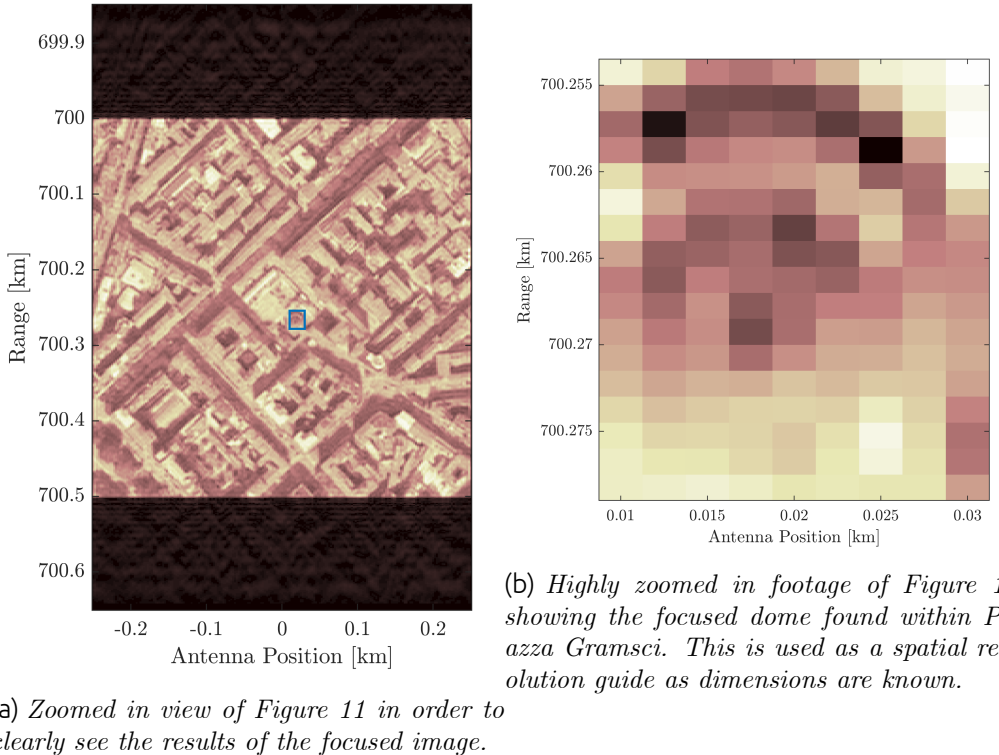


Figure 14: The final focused image for the given input as shown in Figure 5 using the Time Domain Back Projection algorithm.

Finally, comparing the focused images in Figures 13 and 14 shows that from a pure visual inspection

the two algorithms provide similar results with clear distinction between the objects within both images. Only when viewing individual pixels can differences be found. With a requirement of both reasonable accuracy and minimal computational time, this analysis suggests the the ATCC is a better choice between these candidates.

2.3 Evaluate the spatial resolution based on the acquisition parameters described in SAR data and check if it is consistent with the resulting focused image.

The SAR data provides both the system parameters for the satellite along with the range and azimuth resolution. However, for completeness, these equations for these quantities are given by

$$\rho_x = 2\Delta x_{ant} = 5\text{m} \quad (28)$$

$$\rho_R = \frac{c}{2B} = 3\text{m} \quad (29)$$

Using the small dome in the center of *Piazza Gramsci*, as highlighted by the small square within Figures 13a and 14a, which is on the order of $\approx 10\text{m}$ in diameter as a reference point. It can be seen in Figure 13b that the theoretical accuracy is approximately similar to that found practically with the image representing a $20 \times 24\text{m}$ section of the focused image. A more clear representation of the dome is visible within Figure 14b.

References

- [1] Hubert MJ Cantalloube and Carole E Nahum. “Airborne SAR-efficient signal processing for very high resolution”. In: *Proceedings of the IEEE* 101.3 (2013), pp. 784–797.
- [2] Armin Doerry, Edward Bishop, and John Miller. “Basics of Backprojection Algorithm for Processing Synthetic Aperture Radar Images”. In: (Feb. 2016).
- [3] Stefano Tebaldini et al. “Signal Processing Options for High Resolution SAR Tomography of Natural Scenarios”. In: *Remote Sensing* 12.10 (2020), p. 1638. DOI: 10.3390/rs12101638.
- [4] Heng Zhang et al. “An Accelerated Backprojection Algorithm for Monostatic and Bistatic SAR Processing”. In: *Remote Sensing* 10.1 (2018), p. 140. DOI: 10.3390/rs10010140.